Project 2

BAN403: Simulation of Business Processes

Candidate numbers: 142, 180, 186

Handed out: April 7, 2025
Deadline: April 23, 2025

Contents

1 Analyzing the Current Process Design **2**

1.1 Flowchart of the Current X-ray Process 2

1.2 Input Analysis 3

1.3 Simulation Logic for Orderly and Patient Flow 4

1.4 First-Cut Simulation 5

1.5 Simulation with Replications 6

2 Redesign Proposal and Performance Evaluation **7**

2.1 Baseline Process 8

2.2 Redesign 1: Incremental Resource Addition 8

2.3 Redesign 2: Process Restructuring with Digital Imaging 8

3 Comparison and Conclution **9**

4 Reference **10**

Appendix **11**

List of Figures

1 Flowchart 2
2 Fitted Distributions 4
3 Main Simulation 5
4 Structural Redesign 9

List of Tables

1 Baseline and Optimal Resource Configurations for Redesign 1 and Redesign 2 . . 8
2 Comparison of Baseline vs New Design (95% Confidence Intervals) 10

1 Analyzing the Current Process Design

County Hospital has identified its X-ray process as a key candidate for operational improvement. While patients report dissatisfaction with the total time required to complete the procedure, hospital management is concerned with the use of available resources. To address these challenges, we have been asked to analyze the current system and identify opportunities for redesign.

1.1 Flowchart of the Current X-ray Process

The first step towards understanding and improving the process involved creating a visualization of the current system. This is illustrated in the following flowchart:

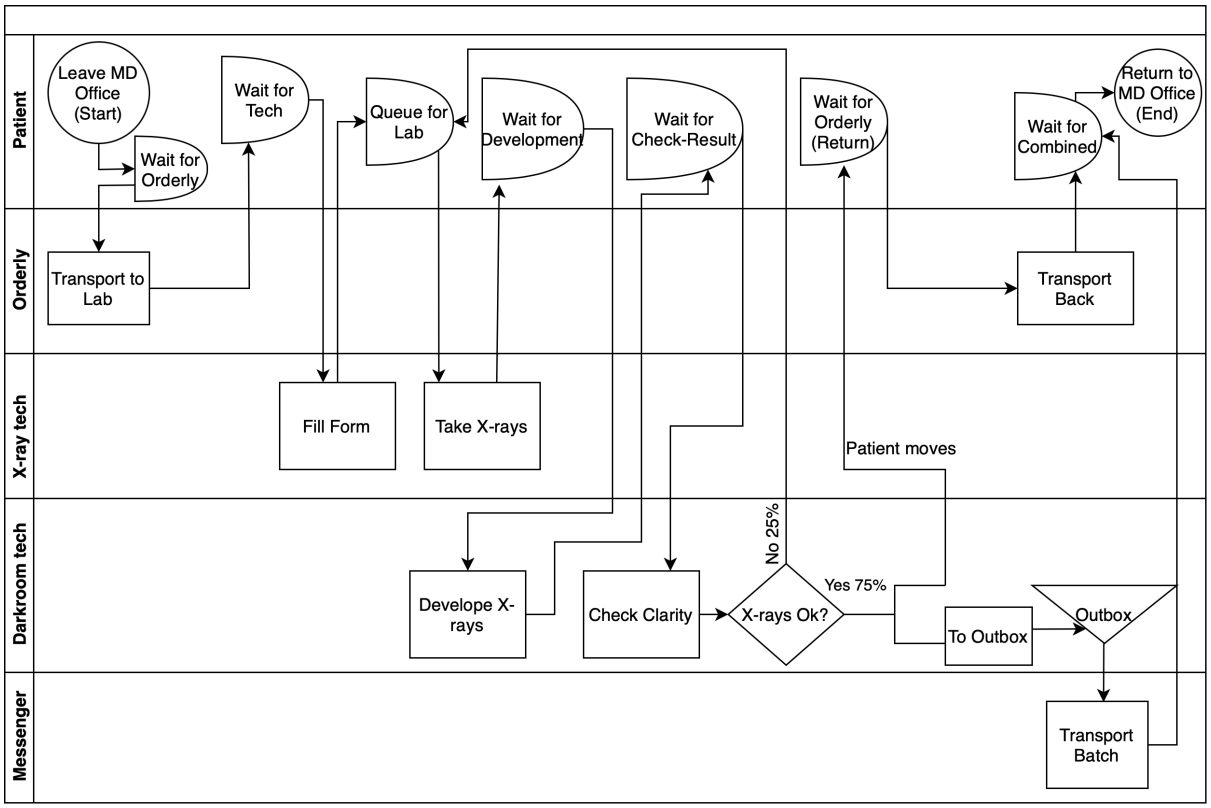

Figure 1: Flowchart

The flowchart is structured using distinct horizontal bands, each corresponding to a key actor or resource group, specifically Patient, Orderly, X-ray Technician, Darkroom Technician, and Messenger. Standard flowcharting symbols are employed to structure the model. (Laguna and Marklund, 2019, Figure 4.3, p.113). Ovals mark the start and end points of the process, while rectangles represent activities. D-shaped symbols indicate unplanned waiting stages arising from resource contention, and a diamond is used for the single decision point that alters the process path. The inverted triangle illustrates the only planned storage in the process, which is the Outbox for batching. Throughout the diagram we also used arrows to indicate the direction and sequence of flow.

The process begins when the patient leaves the physician's office and enters a waiting stage for an available orderly. Once available, the orderly transports the patient to the lab area. Upon arrival, the patient may encounter several unplanned wait stages before and during the imaging process due to limited technician and equipment availability. These include waiting for

a technician, queueing for lab entry, and additional delays introduced in the diagram to reflect potential bottlenecks more realistically.

Specifically, the flowchart includes the waiting points: `Wait for Orderly`, `Wait for Tech`, `Queue for Lab`, `Wait for Development`, `Wait for Check-Result`, `Wait for Orderly (Return)` and `Wait for Combined`. These stages represent points where patients may experience delays due to constrained access to resources. `Wait for Combined` captures the unplanned delay that may occur when the patient and their completed X-rays are not yet simultaneously available for re-entry to the physician's office. Although the messenger is a limited resource, no explicit waiting stage is added, as messenger availability is implicitly accounted for through the batching delay at the Outbox and its downstream effect on patient synchronization.

Following the form completion and X-ray imaging, the darkroom technician develops the X-rays, which are then reviewed for clarity in collaboration with the X-ray technician. If the images are considered unclear (25% probability), the patient re-enters the queue for lab access, repeating the imaging sequence (Activities 5 through 7). If approved (75% probability), the patient proceeds to wait for return transport, while the completed X-rays are sent to the outbox, where they are stored until a batch of five jobs is ready for messenger pickup.

While the case description notes that patient priorities (emergency vs. nonemergency) influence the queue discipline, this flowchart focuses on modeling the core activity sequence and structure. It also simplifies collaborative steps, such as the joint review in Activity 7, and implies physical resource usage within technician bands rather than explicitly modeling all assets as separate bands. These resource constraints, queuing disciplines, and shared resource interactions are fully addressed in the JaamSim simulation developed from this framework.

1.2 Input Analysis

Building on the process structure from the flowchart, the next focus was preparing the required input data. The case description, along with the provided excel file, formed the foundation for modeling variability inherent in the X-ray process. For the unknown distributions of patient arrivals and Activities 4 and 7, we relied on the provided empirical data and descriptive statistics.

The input analysis began with visual inspection of the raw data, followed by a statistical fitting. To evaluate candidate distributions, we applied the Kolmogorov–Smirnov (KS) goodness-of-fit test, which is particularly suited for continuous distributions and provides a formal mechanism to assess the fit between empirical and theoretical models (Laguna & Marklund, 2019, Appendix 9A.1.2, p. 422). Five standard continuous distributions were evaluated, including Exponential, Gamma, Lognormal, Weibull, and Normal. A summary of these candidate distributions and the corresponding fitted results is presented in Figure 2.

The interarrival times were fitted to the candidate distributions, and the best-fitting model differed between emergency and non-emergency patients. The Weibull distribution provided the best fit for emergency arrivals (KS = 0.0370, p = 0.7919), while the Gamma distribution was most appropriate for non-emergency arrivals (KS = 0.0888, p = 0.6985). Acitivity 7 (Clarity Check) was analyzed using the same fitted procedure, and the Gamma distribution again yielded the best statistical fit (KS = 0.0286, p = 0.7967). For Activity 4 (Form Filling), no raw data were provided. However, we were given minimum, maximum, and mode values (Min = 3, Max = 6, Mode = 5 minutes). In such cases, the Triangular distribution is the recommended modeling approach, as it can be fully specified from these three parameters without requiring empirical samples (Laguna and Marklund, 2019, Section 9.2.3, p. 367).

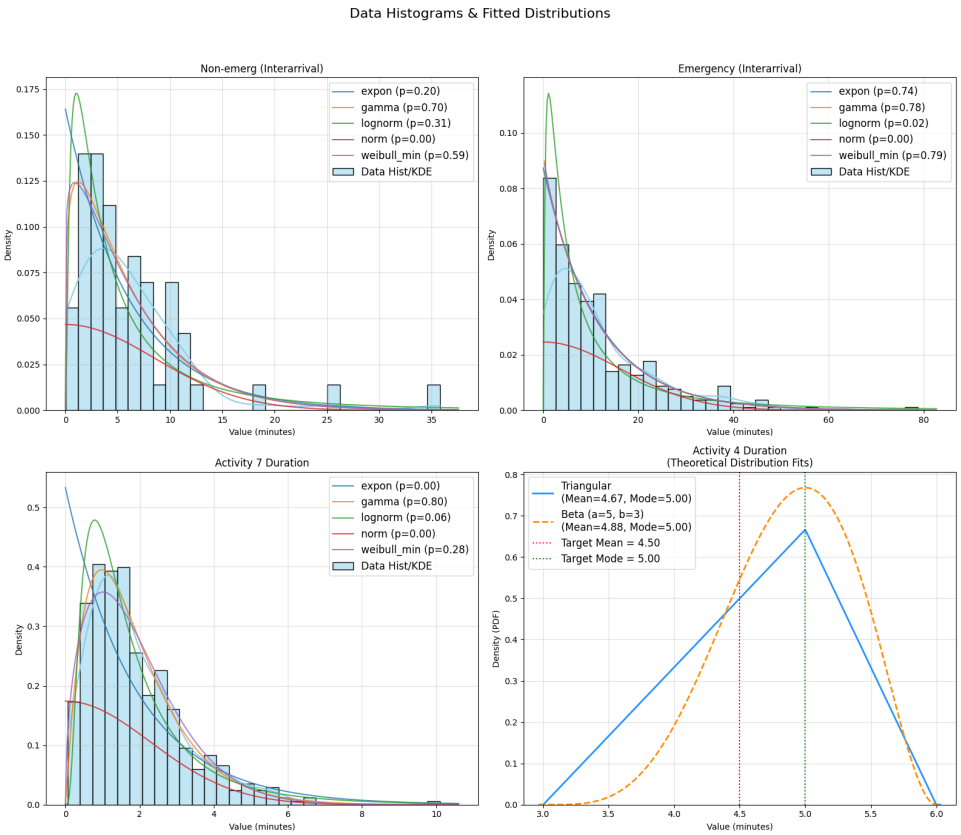

Figure 2: Fitted Distributions

The theoretical mean of the triangular distribution was 4.67 minutes, slightly above the implied target of 4.5 minutes. Given the nature of expert-estimated parameters and the triangular distribution's purpose, modeling processes where only the minimum, maximum, and mode values are known, this level of deviation is within a reasonable range for simulation modeling (Laguna & Marklund, 2019, p. 367). We also explored the Beta distribution as an alternative, but found that it could not simultaneously satisfy both the target mean and mode within the specified range as effectively as the triangular distribution.

1.3 Simulation Logic for Orderly and Patient Flow

The simulation model implements a tightly controlled system for managing patient transport and orderly behavior, designed to satisfy every operational requirement with precision. Particular emphasis was placed on the movement logic of orderlies, the tracking of patient types, and the careful management of resource states through the full cycle of the process.

Each patient arriving at `QueueOrderlyToLab` seizes an orderly resource via a `Seize` object associated with `OrderlyPool`, with a restriction of one unit per transport. This ensures that orderlies are never dispatched without accompanying a patient, strictly enforcing the no-empty-travel constraint. Transportation is modeled by `DelayTransportToLab`, applying a uniform distribution (Act2) dependent on patient type, while ensuring that the orderly remains bound to the patient entity throughout the transit. At the X-ray lab, a `Duplicate` object separates the patient and the orderly into two independent entities. The patient proceeds independently into the examination and X-ray processing stages, while the orderly enters a decision logic sequence to determine return options. Maintaining logical separation at this point allows the model to trace patient flow and resource utilization independently without compromising systemic coherence.

The orderly's return decision is governed by dynamic system conditions monitored through the `DecideReturnTrip` logic. Initially, the orderly evaluates `QueueWaitForOrderlyBack` to check for available patients and inspects the state of `Wait5minGate` to ensure no preemption occurs. If a patient is available and the gate is free, the orderly engages a `Combine` operation, joining with the patient through `OrderlyCombineQueue` and `CombinePatientOrderly` to initiate the return process. The subsequent transport back to the ward is modeled using `PatientBackDelay`, an `EntityConveyor` governed by a uniform distribution (Act10) conditional on patient type, mirroring the stochastic structure applied for outbound travel. If no patient is immediately available, the orderly is directed to `Wait5minGate`, where an `ExpressionThreshold` dynamically monitors patient readiness in the system. This threshold triggers gate release upon the first arrival of a patient within a maximum five-minute waiting period, ensuring that orderlies can adapt responsively to system changes without unnecessary idle time.

If the five-minute waiting threshold expires without a patient becoming available, an empty return is initiated via `OrderlyGoingBack`, modeled with a deterministic five-minute `EntityDelay` representing walk-back time without a patient. Upon completion of the return journey, the orderly releases the seized resource, returning to the `OrderlyPool` and becoming available for new transport assignments. The system employs distinct `Sink` objects to register the completion of orderly trips depending on whether the return was conducted with or without a patient. Specifically, `OrderlyEnd` captures orderlies returning successfully with a patient, while `OrderlyReturnsEmptySink` records empty returns. The use of `Sinks` enables a detailed breakdown of orderly performance, supporting later analysis of resource utilization, idle time, and system efficiency.

An internal tracking mechanism was incorporated through assignment operations immediately following the duplication. This mechanism continuously monitors the patient type associated with entities progressing through the system, identifying if the entity is of emergency or non-emergency status. This dynamic updating is critical for ensuring that subsequent conditional logic, such as transport time selection or statistical output reporting, accurately reflects the patient's classification at each stage of the simulation.

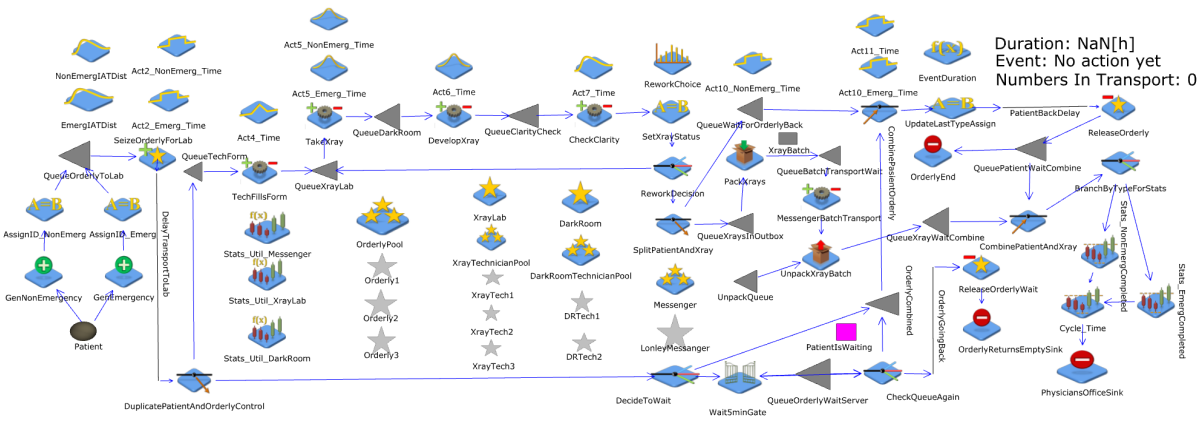

Figure 3: Main Simulation

1.4 First-Cut Simulation

To establish a baseline for the current X-ray process, we conducted a first-cut simulation representing one 12-hour operating day. The process is modeled as a terminating process, as it operates within a fixed 12-hour window from 08:00 to 20:00. The system starts at an empty

state each morning, and any patients not completing the process by closing time are considered unserved and must leave. This bounded timeframe justifies the use of a terminating simulation, as it captures a complete and consistent cycle of daily operations.

The first-cut simulation revealed several critical performance issues. The average patient cycle time was 3.42 hours, and the daily throughput reached only 40 out of 182 arrivals, confirming that the system cannot meet demand under current conditions. Resource and queue statistics indicated that the `DarkRoom` is a bottleneck, operating at 96.32% utilization with an average queue length of 17.7 patients. Limited darkroom capacity delayed the processing flow and created upstream congestion, particularly impacting the `OrderlyPool`, which showed near-complete saturation at 99.92% and an average of 27.4 patients waiting for transport.

The bottleneck effect propagated across other stages. Orderlies were frequently delayed, often returning empty after a five-minute threshold, observed 82 times, reducing transport availability and exacerbating entry delays. Additionally, a resource mismatch emerged at the imaging stage. While `XRayLab` utilization was moderate at 58.66%, the `XRayTechnicianPool` was heavily loaded at 98.56%, suggesting that technician shortages constrained system flow. Queue lengths further confirmed this, with `QueueTechForm` averaging 14.1 patients and `QueueXrayLab` 7.9 patients. Activity utilization patterns highlighted a concentration of technician workload in `DevelopXray` (96.32%) and `TakeXray` (80.30%), while activities such as `TechFillsForm` (53.75%) and `CheckClarity` (15.09%) were underutilized.

Overall, the simulation pointed to systemic bottlenecks driven by darkroom limitations and technician availability imbalances. While these findings offer strong initial insights, they are based on a single run. Replicated simulations are therefore necessary to confirm the reliability of these performance estimates.

1.5 Simulation with Replications

The number of required replications is determined by targeting a 95% confidence interval with a precision of 5% relative to the mean. Based on a preliminary analysis with 10 replications, the sample mean for cycle time was 3 hours with a standard deviation of 1.21 hours, while throughput was 38.30 patients with a standard deviation of 4.24 patients.

The required number of replications n is computed using the formula:

$$n = \left(\frac{z_{\alpha/2} \cdot s}{d}\right)^2$$

where $z_{\alpha/2} = 1.96$ for a 95% confidence level, s is the sample standard deviation, and d is the desired half-width, defined as 5% of the sample mean (Laguna & Marklund, 2019, pp. 386–389).

Applying this methodology, the required number of replications is calculated as 252 for cycle time and 19 for throughput. Since the precision requirement must be satisfied for all performance measures, the higher value of 252, is selected (Laguna & Marklund, 2019, pp. 386–389).

Extending the simulation to 252 replications provides a more statistically reliable characterization of the X-ray process compared to the preliminary first-cut, single-day simulation. The average cycle time decreases to 3.13 hours, with a 95% confidence interval between 3.05 and 3.20 hours, compared to 3.42 hours observed in the single-day analysis. In contrast, the daily throughput remains relatively stable, with 39.85 patients in the full simulation versus 40 patients in the first-cut simulation. This discrepancy in cycle time highlights the risks associated with drawing conclusions from limited simulation horizons, where short-run variability and random

favorable conditions may temporarily conceal systemic congestion effects (Laguna & Marklund, 2019, pp. 386-389).

Resource utilization patterns provide deeper insight into the structural challenges of the system. The `Orderly Pool` operates at 100% utilization, and the `X-ray Technician Pool` at 99%. The `DarkRoom` activity also exhibits critically high utilization at 96%, although the `DarkRoom Technician Pool` maintains only moderate utilization at 55%. This indicates that the primary constraint emerges from a combination of physical limitations at the `DarkRoom` and the intensive demand placed on `X-ray Technicians`, who support multiple sequential activities including `TechFillsForm`, `TakeXray`, `DevelopXray`, and `CheckClarity`. As the `DarkRoom` depends on technician availability, it becomes the point where these resource constraints converge most visibly. The resulting bottleneck reflects systemic interdependencies across activities and shared human resources rather than isolated capacity restrictions.

Further examination of queue metrics substantiates this structural interpretation. The average queue length for transport to the X-ray Lab increased from 27.44 patients in the first-cut simulation to 28.43 patients in the full simulation. Likewise, the queues at the `X-ray Lab` and the `DarkRoom` remained substantial, stabilizing at 7.53 and 17.45 patients, respectively. The persistence of sizeable queues, particularly upstream of capacity-constrained resources, illustrates the classic effects of resource contention, where bottlenecks at critical stages create upstream blockages and sustained system-wide delays (Laguna & Marklund, 2019, p. 130).

Overall, the extended simulation confirms and refines the insights drawn from the first-cut analysis. The X-ray process is shaped by structural bottlenecks arising from the combined effects of limited `DarkRoom` capacity and the intensive multi-tasking load placed on `X-ray Technicians`, who support several critical activities. These constraints are further compounded by coordination inefficiencies in patient transport. Sustainable improvements in throughput and cycle time require addressing these interdependent limitations holistically, rather than treating individual stations or resources in isolation.

2 Redesign Proposal and Performance Evaluation

This study proposes and evaluates redesign strategies for the X-ray department to reduce patient cycle time and increase daily throughput. The approach integrates discrete-event simulation using JaamSim with optimization modeling formulated as a mixed-integer linear programming (MILP) problem, solved in Pyomo with the CBC solver. Alternative configurations are assessed through scenario-based simulation experiments and statistical output analysis, including the construction of confidence intervals to ensure the reliability of performance estimates. The objective is to minimize cycle time and improve daily throughput while maintaining operational feasibility and cost-effectiveness. The estimates are calculated as annual costs by multiplying the number of resources by their annual unit cost, based on publicly available data from sources such as Glassdoor, All Allied Health Schools, and DataUSA, without accounting for overtime, employer contributions, or other additional costs.

The total annual operating cost, which serves as the objective function for the forthcoming optimization models, is minimized as follows:

$$\text{Minimize} \quad Z = \sum_{r \in R} (BaseRes_r + x_r) \times Cost_r \tag{1}$$

Table 1: Baseline and Optimal Resource Configurations for Redesign 1 and Redesign 2

Resource	**Baseline**	**Redesign 1**	**Redesign 2**
Orderly	3	4	5
X-ray Technician (XRT)	3	5	6
Darkroom Technician (DRT)	2	5	–
Messenger	1	1	–
X-ray Lab	2	3	4
Darkroom	1	4	–

2.1 Baseline Process

The baseline simulation model captures the current X-ray process, with patient flow through orderly transport, X-ray acquisition, darkroom development, and final discharge. Based on replicated simulation runs, the average patient cycle time was estimated at 3.42 hours, with a daily throughput of approximately 40 patients. Based on standard unit costs, the total estimated annual operating cost for the baseline configuration is $999,000. This cost structure, alongside the observed throughput constraints and resource bottlenecks, forms the foundation for the redesign evaluations that follow.

2.2 Redesign 1: Incremental Resource Addition

The first redesign strategy improves system performance by combining incremental resource additions with a minor process adjustment, where the X-ray technician (XRT) is no longer required during the `DevelopXRay` and `CheckClarity` activities. This modification allows XRTs to return to new patients immediately after image acquisition, increasing technician availability and reducing idle time. A full-factorial simulation experiment evaluated 4,096 configurations by varying the addition of up to three units across six resource types: orderlies, XRTs, darkroom technicians (DRTs), messengers, X-ray labs, and darkrooms. Each configuration was simulated under terminating conditions with multiple replications to ensure statistical validity. Based on the simulation results, a mixed-integer linear programming (MILP) model was formulated to identify the cost-minimizing configuration that achieves at least 95% of the maximum observed throughput. The optimization results are summarized in Table 1.

Redesign 1 achieves an estimated daily throughput of approximately 144 patients, with a total annual operating cost of $2,003,700. The corresponding average patient cycle time improved to 2.95 hours, reflecting the combined effects of enhanced technician availability and expanded processing capacity. Although the technician decoupling improves resource utilization, substantial expansion of darkroom capacity remains necessary to meet the required throughput under the existing process structure.

2.3 Redesign 2: Process Restructuring with Digital Imaging

To overcome limitations inherent in the darkroom process, the second redesign restructures the X-ray process through the adoption of digital imaging technology. The removal of darkroom development, physical film handling, and manual transport eliminates non-value-adding activities that contributed to synchronization delays and process inefficiencies (Laguna and Marklund, 2019, s. 169). In the reengineered workflow, digital images are immediately available upon acquisition, minimizing intermediary handling steps, reducing process variability, and improving overall resource synchronization.

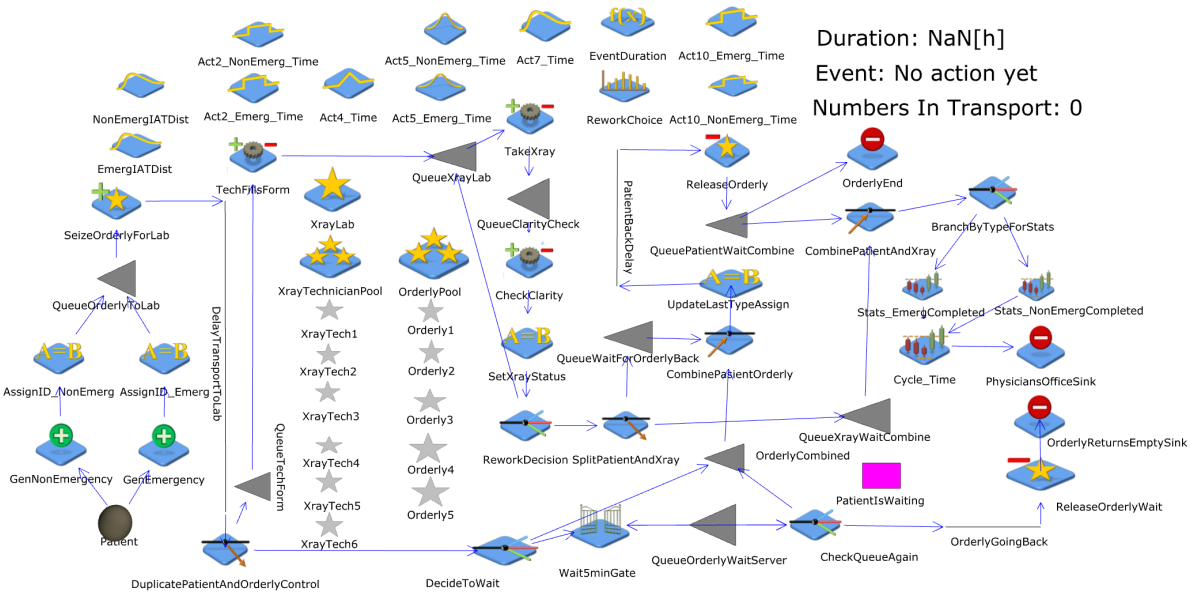

Figure 4: Structural Redesign

The analysis assumes that the new X-ray machines incur the same recurring operating costs as the existing ones, and excludes any capital investment costs. In addition, training expenses are considered one-time costs and are therefore not included in the annual estimates. It is also assumed that staff are willing and able to adapt to new roles as part of the redesign.

Personnel previously assigned to obsolete tasks are strategically redeployed. Darkroom Technicians (DRTs) are retrained to expand the pool of X-ray Technicians (XRTs), supporting the increased demand for imaging activities without requiring external recruitment. Messenger staff are retrained as Orderlies, aligning workforce capabilities with the demands of patient transport within the streamlined digital workflow. This reallocation approach preserves institutional knowledge and supports a smooth transition to the new system design.

A discrete-event simulation evaluated 343 alternative configurations by varying the number of Orderlies, XRTs, and X-ray Labs. A mixed-integer linear programming (MILP) model identified the cost-minimizing configuration that achieved at least 95 percent of the maximum observed throughput.

Redesign 2 achieves an estimated daily throughput of 164 patients, an annual operating cost of $1,379,000, and an average patient cycle time of 1.04 hours. Although total annual costs increase by approximately $380,000 relative to the baseline, the significant increase in throughput leads to a substantial reduction in the unit cost per patient. This confirms that technology-enabled process restructuring not only improves operational efficiency and reduces cycle times but also enhances economic performance by lowering the cost per service delivered.

3 Comparison and Conclution

Table 2 compares the baseline process with the significantly improved performance from Redesign 2, evaluated at the 95% confidence level. The required number of replications was determined using the same procedure as in Task 2, resulting in 333 replications.

Table 2: Comparison of Baseline vs New Design (95% Confidence Intervals)

Metric	Baseline Mean	Baseline 95% CI	Redesign 2 Mean	Redesign 2 95% CI	% Change
Cycle Time (min)	187.52	[183.01, 192.03]	62.27	[61.24, 63.30]	-66.8%
Throughput (patients)	39.85	[39.32, 40.38]	163.79	[162.73, 164.84]	+311.1%
Orderly Utilization	1.00	[1.00, 1.00]	0.81	[0.81, 0.82]	-18.5%
Technician Utilization	0.99	[0.98, 0.99]	0.84	[0.84, 0.85]	-14.3%
Xray Lab Utilization	0.61	[0.61, 0.62]	0.83	[0.82, 0.83]	+34.8%
Queue Time to Lab (min)	111.23	[108.75, 113.71]	4.52	[4.15, 4.90]	-95.9%
Queue Time for Tech Form (min)	78.74	[77.58, 79.89]	0.95	[0.89, 1.01]	-98.8%
Queue Time at Xray Lab (min)	49.57	[48.49, 50.65]	5.37	[4.87, 5.87]	-89.2%
Queue Time for Clarity Check (min)	9.51	[8.77, 10.25]	1.06	[0.99, 1.13]	-88.9%

The redesigned process demonstrates a substantial improvement in both cycle time and throughput. The average cycle time is reduced by approximately 66.8%, from 187.5 minutes to 62.27 minutes. This reduction is statistically significant, as confirmed by non-overlapping confidence intervals. According to Little's Law, a reduction in average time in the system directly correlates with reductions in waiting times and increases in system efficiency for a given arrival rate (Laguna & Marklund, 2019, p. 157). This is further reflected in throughput, which increased by 311%, from 39.85 to 163.79 patients per day.

Resource utilization metrics reinforce the conclusion that the redesign enhanced systemic balance and resilience. Orderly utilization declined from full saturation at 1.00 to 0.81, mitigating the risks associated with resource exhaustion and unstable queuing dynamics. Technician utilization also experienced a notable reduction from 0.99 to 0.84, indicating a gain in operational flexibility without introducing significant idle capacity. Concurrently, X-ray lab utilization increased from 0.61 to 0.83, reflecting a more efficient use of critical, high-cost resources, a key consideration in capacity-constrained settings (Laguna and Marklund, 2019, p. 171).

Queue performance showed substantial improvements across all key activities. The average waiting time to access the lab area decreased by over 95%, with similarly large reductions in other queue times. These results are consistent with queuing theory, where reducing variability and eliminating non-value-adding tasks shorten queues and waiting times.

In conclusion, the redesigned process demonstrates statistically and operationally significant improvements relative to the baseline in terms of cycle time, throughput, resource utilization, and queuing performance. The evidence strongly supports that these improvements are structural and not attributable to random variation. Although the increase in queue time for the clarity check warrants further monitoring, it does not materially offset the substantial gains in system efficiency and patient flow achieved through the redesign.

4 Reference

Laguna, M., & Marklund, J. (2019). *Business Process Modeling, Simulation and Design* (3rd ed.). CRC Press.

Appendix

This section provides an overview of the supplementary files contained in `Simulations-att-proj2.zip`, submitted with this report.

- **Task2_Jaamsim folder**: Contains our first JaamSim `.cfg` file for the initial simulation, as well as the flowchart presenting the current X-ray process.
- **Task3_Jaamsim folder**: Containts our Jaamsim `.cfg` files related to the redesign proposal.
- **Simulations.ipynb**: This Jupyter Notebook includes all scripts used for input data analysis and output processing to support the conclusions presented in this report.
- **Data folder**: Contains the data files used throughout the `Simulations.ipynb` notebook.